Premonsoon Drought in India Observed from Space

W. TIMOTHY LIU AND XIAOSU XIE

Jet Propulsion Laboratory, California Institute of Technology, Pasadena, California

(Manuscript received 5 January 2016, in final form 22 September 2016)

ABSTRACT

Satellite observations between 2007 and 2015 are used to characterize the annual occurrence of the premonsoon drought (PMD), which causes human death and economic hardship in India, and to postulate its scientific causes. The PMD is identified as the driest and hottest weeks in central India just before the summer monsoon onset. The onset is marked by a sharp increase in precipitation and soil moisture and a decrease in air temperature. The difference between integrated moisture transported in from the Arabian Sea and out to the Bay of Bengal is largely deposited as rain over land during the summer monsoon. The PMD occurs during the short period when moisture is drawn out to the Bay of Bengal before it can be replenished from the Arabian Sea. The time gap is caused by the earlier start of summer monsoon (southwest) winds in the Bay of Bengal than in the Arabian Sea. Sea surface temperature rise precedes the start of summer monsoon wind in both the Arabian Sea and the Bay of Bengal, and it has the potential to give advance warning of the PMD and thus allow mitigation of the adverse effects.

1. Introduction

In June 2015, news organizations around the world reported more than 2300 fatalities in the extremely hot and dry weather as people in India waited for the monsoon rain. There were similar anecdotal reports in previous years of extremely dry weeks before the rainy season with associated hot weather, but there is little scientific documentation and few explanations on the cause. The premonsoon drought (PMD) we address in this study is a layman's term, commonly used in the media to describe the short (approximately 2 or 3 weeks), disaster-prone dry periods before the onset of the summer monsoon in a vast region encompassing several states in the central and eastern part of the Indian subcontinent.

There were scientific studies on droughts before monsoon, but they were largely confined to interannual anomalies and long-term trends of the dry (premonsoon) season from March to May, before the wet (monsoon) season from June to September. These studies include those by Gadgil et al. (2007), who linked the rainfall anomalies of the dry and wet seasons to climate indices; by Pal and Al-Tabbaa (2009), who examined five decades of precipitation extremes at Kerala in the dry season as an indicator of long-term climate changes; by Dawadi et al. (2013), who examined almost five centuries of tree-ring records in the Himalayas to establish correlations between dry and wet season rainfall and temperature; and by Thomas and Prasannakumar (2016), who used 141 years of meteorological data to discuss the long-term trend of rainfall of dry and wet seasons in Kerala. Kerala is a state at the southwest of India. These studies did not address the PMD defined by us. Drought is often defined in scientific terms as interannual and longer-term anomalies, such as the Palmer drought severity index or the Standard Precipitation Index (Guttman 1999; Dai et al. 2004). The short durations of satellite data do not allow us to sufficiently examine interannual anomalies and long-term trends. Our PMD may not meet the general scientific definition of drought.

Although drought is always identified by rainfall, rainfall measured by satellite sensors alone does not fully describe the variability of the dryness in the dry season; evaporation/transpiration may add to the variability. For months before the summer monsoon onset, there is practically no consistent rainfall in the central part of India, but strong variability of dry weather is encountered. Surface soil moisture measured by newly available L-band microwave radiometers helps to

Corresponding author e-mail: W. Timothy Liu, w.t.liu@jpl.nasa.gov

DOI: 10.1175/JHM-D-16-0014.1

identify the short period of the PMD in the dry season. Section 2 gives a summary of space-based data. Using these data, the PMD is characterized in section 3.

There are over a century of monsoon onset records, as rainfall around Kerala, transport from the Arabian Sea, and the statistical analyses of these two parameters (e.g., Ananthakrishnan and Soman 1988). For more than half a century, many definitions of monsoon onset and hypotheses on its physical causes have been proposed; the temporal–spatial evolution, the intraseasonal and interannual variability, the regional drive, and the global teleconnection have been analyzed and modeled [see Ramage (1971), Chang and Krishnamurti (1987), and Webster et al. (1998) for reviews].

We begin our study with the classical view of summer monsoon as the supply of ocean moisture to land resulting from seasonal reversal of persistent wind direction (e.g., Ramage 1971; Fasullo and Webster 2003) through the integrated moisture transport. The space-based estimation of the transport is described in section 4. The transport is used as an indicator of the water balance over land in the summer monsoon in section 5. The time difference of monsoon onsets between the two coasts is presented as our hypothesis of the cause of the PMD in section 6.

Near the end, we support our hypothesis through another perspective of summer monsoon onset. The starts of southwest (summer monsoon) wind over Arabian Sea and Bay of Bengal follow the seasonal northward migration of intraseasonal organized convection, which is linked to the ocean heat source and the atmospheric vertical instability. Lau and Yang (1997), Wang et al. (2004), and others, based on convection and rain data, showed a progression of monsoon onset starting first in the South China Sea, then moving to Indochina and the Bay of Bengal. Gadgil (2003) and others have long supported the definition of the Indian monsoon as the manifestation of the seasonal migration of the intertropical convergence zone. The linkage of wind and sea surface temperature (SST) change was presented by Yu et al. (2012), who showed that the surface winds measured at an array of moorings along 90°E (the Bay of Bengal), from 2007 to 2011, changed direction right after the SST peaked. Li et al. (2012), based on outgoing longwave radiation, postulated that during boreal summer, intraseasonal convective systems propagate eastward in the equatorial Indian Ocean and then move northward into the Bay of Bengal to trigger the southwest monsoon. Jiang and Li (2011) showed the relation between SST rise and change of surface winds in both the Arabian Sea and the Bay of Bengal, using 23 years (1986–2008) of climatological averages. Our analysis of 9 years of SST rise and change of moisture transport direction off the east and west coasts of India is presented in section 7, to support our hypothesis that the PMD coincides with the time difference between monsoon onsets on the two coasts.

2. Space-based data

In this study, all data are first averaged over 5-day (pentad) and 0.5° latitude × 0.5° longitude bins for application, regardless of the resolution of the original data we acquired. Our results depend only on how the data vary within each year, and our conclusion does not depend critically on the absolute value and the interannual variability of these measurements. We made no effort to validate and harmonize the data on rainfall and soil moisture measured by different sensors in 2015 with those from the previous 3 years, in addition to efforts by the data providers.

As explained in section 1, space-based measurement of soil moisture is a useful indicator of the PMD in a dry season with little rainfall. Soil moisture is a fraction, defined as volume of water over total volume (water + air + solid). Soil moisture has been retrieved from C-band active and passive sensors, such as the Advanced Scatterometer (ASCAT; Bartalis et al. 2007; Naeimi et al. 2009) and the Advanced Microwave Scanning Radiometer (AMSR) for Earth Observing System (AMSR-E; Jackson et al. 2010). There are ongoing efforts to retrieve soil moisture from WindSat and the Tropical Rainfall Measuring Mission (TRMM) Microwave Imager (TMI; Li et al. 2010). Much of recent efforts have been devoted to retrieving soil moisture from L-band sensors, such as the Soil Moisture Ocean Salinity (SMOS), *Aquarius*, and the Soil Moisture Active Passive (SMAP) missions (Entekhabi et al. 2010; Jackson et al. 2012). They measure soil moisture at a deeper depth (5 cm), compared with 1 cm for AMSR and 2–3 cm for ASCAT. They have a better penetration through vegetation than all other types of sensors. There are ongoing efforts to compare satellite soil moisture products (Burgin et al. 2016, submitted to *IEEE Trans. Geosci. Remote Sens.*). Only *Aquarius* and SMAP are used in this study because they have similar data processing procedures with respect to radio interference and are more consistent over the Indian subcontinents than other data. *Aquarius* data were available from August 2011 to April 2015, and its level-3 soil moisture data at daily and 1° resolutions (Bindlish et al. 2015) were acquired to cover three monsoon seasons in this study. *Aquarius* failed in April 2015, and SMAP data became available just in time to replace *Aquarius* for the monsoon onset of 2015, as shown in Fig. 1. Daily SMAP level-3 radiometer data (Entekhabi et al. 2014) in ease

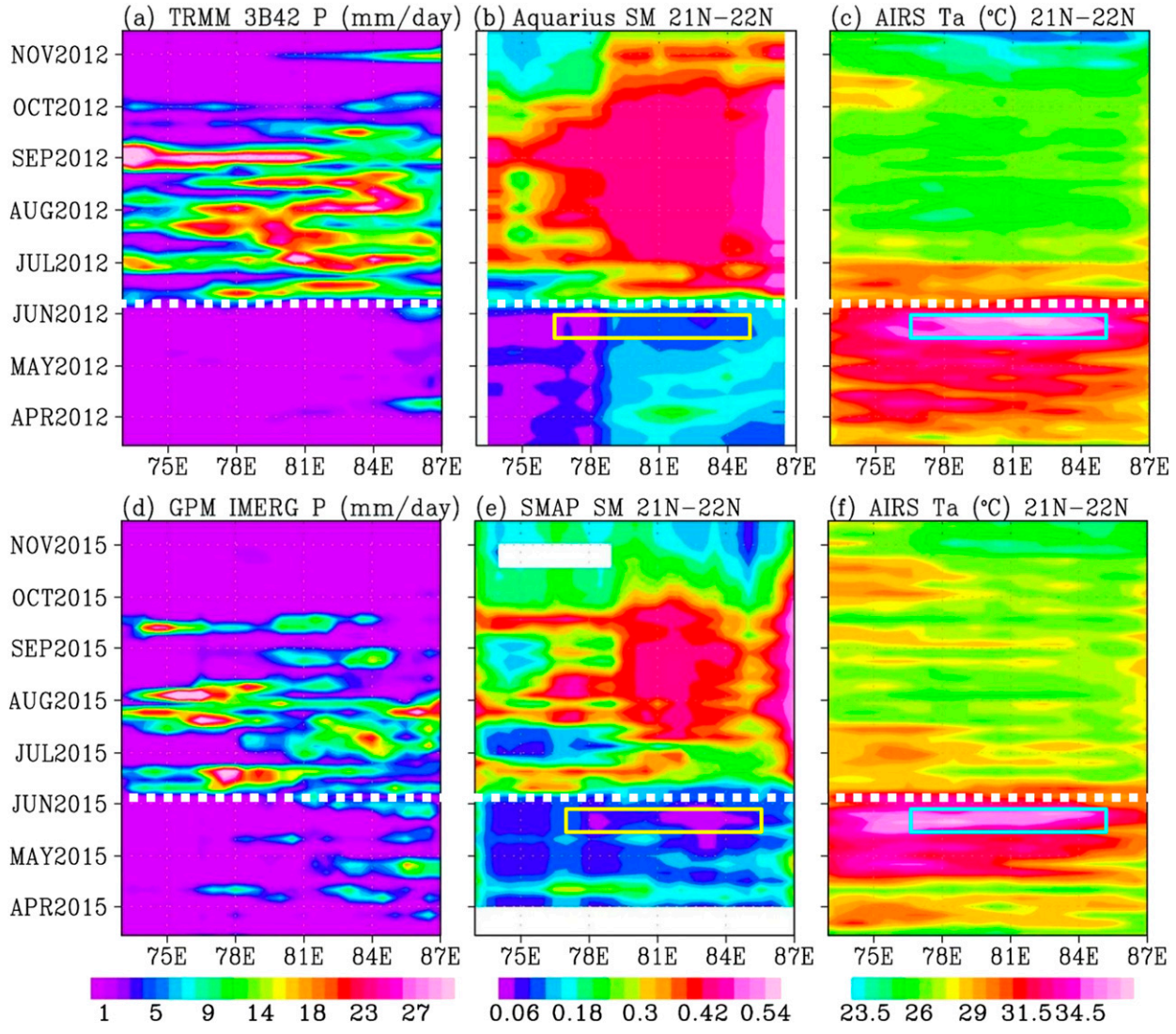

FIG. 1. Time–longitude cross sections of (a) precipitation (mm day^{-1}) from TRMM, (b) soil moisture (fraction) from *Aquarius*, and (c) air temperature (°C) from AIRS, between 21° and 22°N. The data are 5-day average between April and October 2012. (d)–(f) As in (a)–(c), but for 2015 with rain and soil moisture data from GPM and SMAP. White broken lines and colored rectangles help to identify monsoon onset and premonsoon drought.

grid (resolution varies with latitude) were acquired to cover the summer monsoon season in 2015.

Surface air temperature is measured by the Atmospheric Infrared Sounder (AIRS), which has provided temperature and humidity profiles in the atmosphere with accuracy comparable to those of conventional radiosondes since 2002 (Chahine et al. 2006). In this study, data from version 6 of AIRS level-3 standard gridded products with 1° and daily resolution from the Goddard Earth Sciences Data and Information Services Center are used.

TRMM measured precipitation rate from December 1997 until it was terminated in April 2015, covering both ocean and land from 40°S to 40°N. Data from the Global Precipitation Measurement (GPM) mission, with global coverage, were used for the 2015 summer monsoon season. The TRMM 3B42 data at daily and 0.25° resolution (Huffman et al. 2007) and the Integrated Multisatellite Retrievals for GPM (IMERG) data at 30 min and 0.1° resolution (Huffman et al. 2014) combining microwave and infrared precipitation estimates are used to compute surface rainfall over the India subcontinent. The merged data products are produced by the GPM flight project with extensive ongoing validation and comparisons.

SST data used in this study are from TMI up to mission termination in April 2015 and then replaced by those derived from the Advanced Microwave Scanning

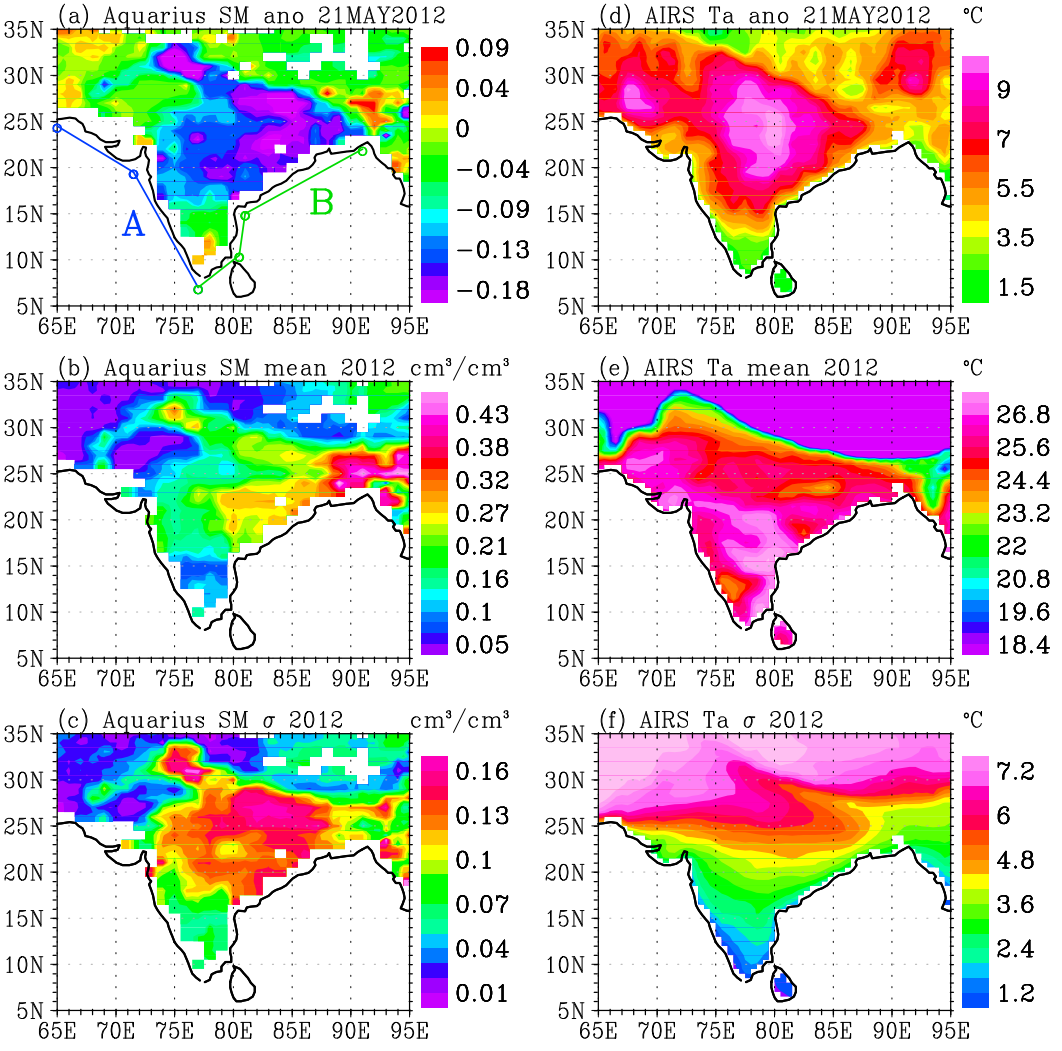

FIG. 2. (a) Soil moisture anomaly (deviation from annual mean) for the pentad starting on 21 May 2012, (b) annual mean of 2012, and (c) std dev of 2012. (d)–(f) As in (a)–(c), but for air temperature. Letters *A* and *B* in (a) mark simplified coastlines for moisture transport analysis in Fig. 4.

Radiometer 2 on Global Change Observation Mission–Water (GCOM-W) to cover the monsoon season in 2015. SST data from both sensors are produced at a 0.25° grid for ascending and descending paths and are validated by Remote Sensing Systems (Wentz et al. 2001).

3. Characterization of premonsoon drought

Figure 1 shows the longitude–time variations of rainfall, soil moisture, and surface air temperature, averaged between 21° and 22°N, across the middle of the Indian subcontinent, from mid-March to mid-November, from the Arabian Sea to the Bay of Bengal. Over these latitudes, the largest ratios are found for the deviation of the soil moisture from the annual mean to the annual standard deviation. In both years (2012 and 2015), shown here as examples, the hottest and driest weeks are found before the summer monsoon starts in June, and they represent the PMD. Similar variations are found in 2013 and 2014 (not shown). We include 2015 analysis to show that, even with different sensors for soil moisture and rainfall, results similar to previous years are produced.

In Fig. 2, the distribution of the deviation from the yearly mean (anomaly) for soil moisture and air temperature during the PMD in 2012 is shown with those for the yearly mean and standard deviation as an illustration of the extent of the dryness and hot temperature during that pentad. The extreme dry area covers the Telangana and Odisha states, where

TABLE 1. Four parameters during PMD for 4 years. The starting date of the pentad, the soil moisture anomaly (SMA), the ratio of SMA to the yearly standard deviation (SMA/std dev), the air temperature anomaly (ATA), and ratio of ATA/std dev are shown. The anomaly is the deviation from the yearly mean.

Date	SMA ($cm^3\ cm^{-3}$)	SMA/std dev	ATA (°C)	ATA/std dev
21 May 2012	−0.217	−1.60	11.5	2.78
6 May 2013	−0.247	−1.89	11.4	2.89
21 May 2014	−0.242	−1.69	10.2	2.11
21 May 2015	−0.176	−1.35	10.9	2.10

weather-related fatalities were reported. The low soil moisture and high temperature anomalies are absent at the southern tip of the subcontinent, where monsoon rain starts early. The distributions in 2013–15 are similar. Soil moisture and air temperature anomalies and the ratio of anomalies to yearly standard deviation at a pentad during the PMD for 4 years are listed in Table 1.

4. Integrated moisture transport

The computation of integrated moisture transport

$$\mathbf{\Theta} = \int_0^{p_s} q\mathbf{u}\, dp,$$

where p is the pressure, p_s is the pressure at the surface, and q and $\mathbf{u}$ are the specific humidity and wind vector at a certain level, depends on the vertical profile of $\mathbf{u}$ and q, which are not measured from space directly. Statistical models were developed to relate $\mathbf{\Theta}$ to the equivalent neutral wind measured by QuikSCAT, cloud-drift winds at 850 mb from the National Environmental Satellite, Data, and Information Service (NESDIS), and the integrated water vapor measured by the Special Sensor Microwave Imager (SSM/I), based on support vector regression (Xie et al. 2008). The addition of cloud drift wind to account of the vertical variability of wind was an improvement on an earlier method (Liu and Tang 2005). The significance of the improvement was best demonstrated by Liu et al. (2012) in the study of ocean influence on West African rainfall, where the surface winds are in a different direction from winds aloft. The $\mathbf{\Theta}$ derived from our improved method agrees with $\mathbf{\Theta}$ derived from 90 rawinsonde stations from synoptic to seasonal time scales and from equatorial to polar oceans (Xie et al. 2008). Hilburn (2010) found very good agreement between our dataset and data computed from the Modern-Era Retrospective Analysis for Research and Applications (MERRA) over the global ocean. Liu et al. (2006) used the data to achieve closure of water balance for the continent of South America. Further evaluation of the divergence of $\mathbf{\Theta}$ as the surface water flux was presented by Liu and Xie (2014). In this study, the surface wind vector from ASCAT, available from 2007, was used to replace QuikSCAT.

5. Relating Θ with monsoon

A good way to study monsoon onset is through $\mathbf{\Theta}$. The component of $\mathbf{\Theta}$ normal to the simplified coastline A of the Arabian Sea (positive onshore and negative offshore) is integrated along the coastline. The correlation coefficients of the monthly-mean time series of integrated $\mathbf{\Theta}$ and the precipitation measured by TRMM over the subcontinent, for the period between March 2007 and May 2015, are shown in Fig. 3. TRMM data after May 2015 are not available. Assuming the 99 months of data are independent, a correlation coefficient higher than 0.22 would meet the 95% confidence level. The seasonal variation of rain over India is significantly correlated to the moisture imported from the Arabian Sea, except for a small region in Tamil Nadal, opposite to Sri Lanka.

Four years (2012–15) of $\mathbf{\Theta}$ integrated along the simplified coastlines of the Arabian Sea and along the Bay of Bengal, shown as A and B in Figs. 2a and 3, are compared in Fig. 4a. The $\mathbf{\Theta}$ is projected normal to the coastline, positive directed from ocean to land and negative from land to ocean. Starting between May and

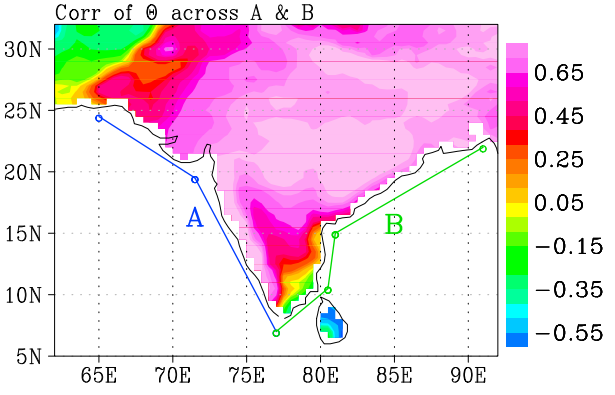

FIG. 3. Correlation coefficient between $\mathbf{\Theta}$ across simplified coastline A and precipitation derived from TRMM 3B42, between March 2007 and May 2015. The $\mathbf{\Theta}$ is positive directing on shore and is derived according to the procedure by Xie et al. (2008), using ASCAT and other data.

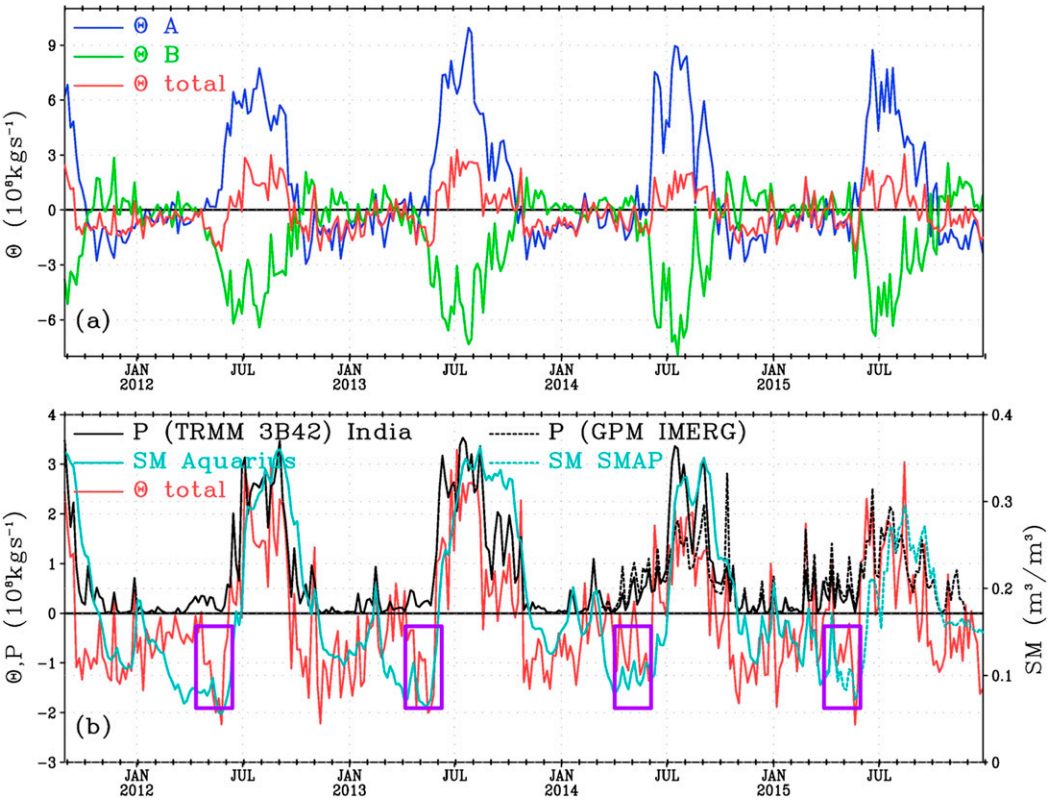

FIG. 4. (a) Time series of **Θ** from the Arabian Sea to land integrated along coastline *A* (blue), **Θ** from the Bay of Bengal to land integrated along coastline *B* (green), positive for onshore flow, and the net transport to land (red), computed by subtracting green line values from blue line values. (b) Time series of spatially integrated precipitation (black) and averaged soil moisture (cyan), over land bounded by 10°–30°N, 72°–85°E, and net **Θ** (red) from (a). Coastlines *A* and *B* are delineated in the map of Fig. 2a.

June, when **Θ** at the coast of the Arabian Sea turns sharply positive, summer rainfall starts, and **Θ** at the coast of the Bay of Bengal turns negative. The direction of transport is reversed for the rest of the year. The net transport in Fig. 4a (sum of **Θ** across the two coasts) is expanded in Fig. 4b and shown with the total rainfall integrated over the land area bounded by 10° and 30°N, between 72° and 85°E. During the summer monsoon season from June to September, the difference between transports in and out of the subcontinent largely falls out as rainfall. The rainfall and moisture influx agree approximately in magnitude and in phase. Transport across the northern boundary is likely to be small because of the high mountains of the Himalayas. Transports over land to Bangladesh in the east and to Pakistan in the west are not accounted for and would be a cause of any discrepancy. High soil moisture averaged over the land area is also found in the periods of high rainfall. A slower variation in soil moisture than in rain can be discerned, showing water retention by the soil. Soil moisture rises with rainfall, but it does not drop as sharply as rainfall, in general. There is soil moisture variation even without rain, and it is an appropriate drought indicator.

6. Difference in transport across two coasts

Just before the summer monsoon rain starts, the net transport is negative; there is more moisture moving out to the Bay of Bengal than coming in from the Arabian Sea, with low soil moisture (marked by boxes in Fig. 4b). Similar negative moisture influx before monsoon onsets was observed by Liu et al. (2005) for the years 2002 and 2003. During the PMD, moisture is drawn out to the Bay of Bengal before it is replenished by moisture from the Arabian Sea. Examples of the difference in transport during the PMD between the two oceans are demonstrated in Figs. 5a and 5b. In the pentad starting on 16 May 2012, the onshore component of **Θ** from the Arabian Sea is weak, but **Θ** out to the Bay of Bengal is very strong (Fig. 5a). A similar difference is seen in the pentad starting 6 May 2013 (Fig. 5b). An exception is found at the southern tip of the subcontinent. The surface winds from reanalysis of the European Centre for Medium-Range Weather Forecasts (ECMWF), in Figs. 5c and 5d, show that the transport out to the Bay of Bengal may draw dry air from the northwestern part of

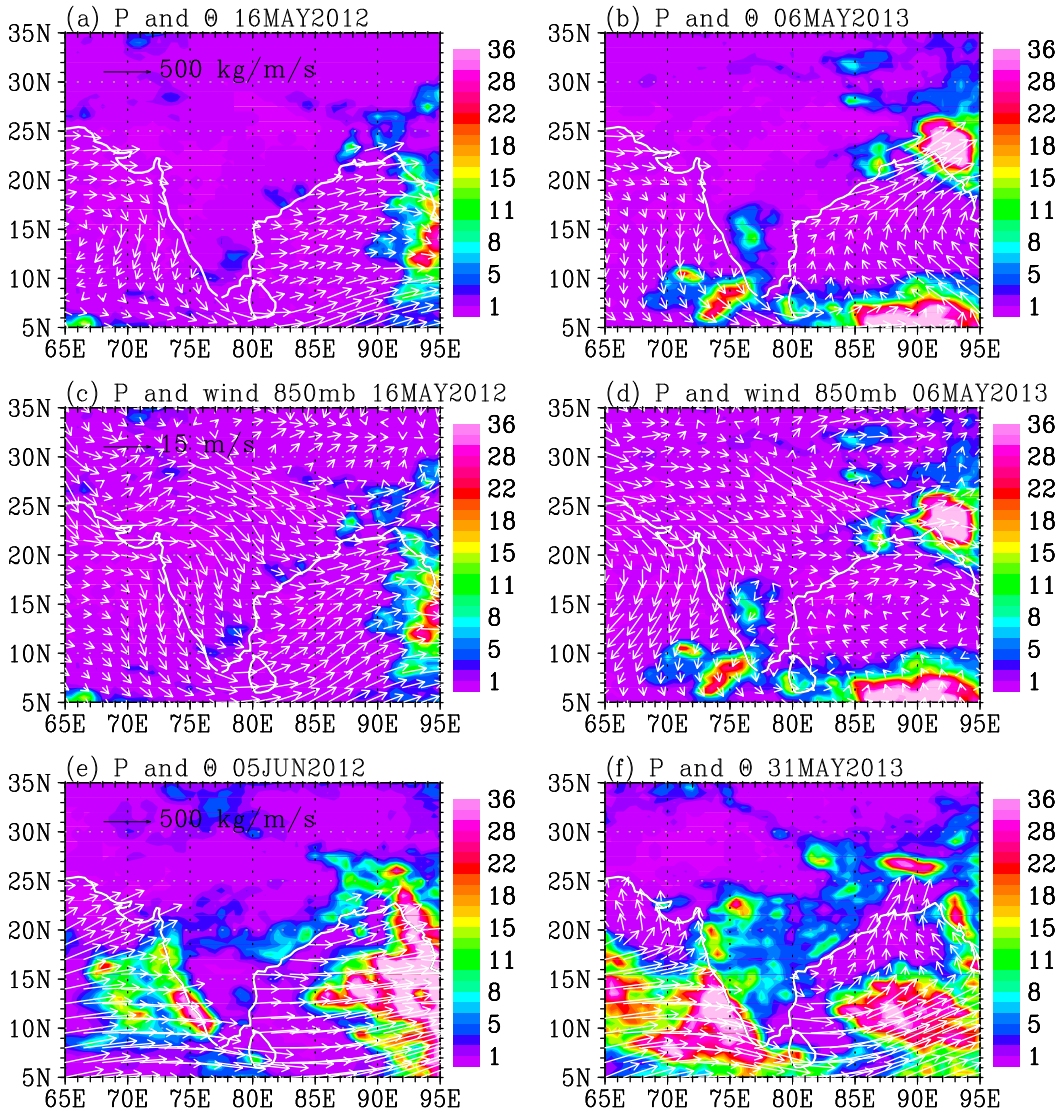

FIG. 5. (a) The **Θ** and (c) 850-mb wind (white arrows), averaged for the pentad starting on 16 May 2012, superimposed on precipitation (color shading). (b),(d) As in (a),(c), but for the pentad starting on 6 May 2013. (e),(f) As in (a), but for the pentad starting on 5 Jun 2012 and 21 May 2013, respectively.

India. Several pentads later, summer monsoon was in full swing on the subcontinent, with **Θ** coming in from the Arabian Sea and going out to the Bay of Bengal (Figs. 5e,f). Figures 5a and 5b also indicate that **Θ** from the east starts early all along the equatorial ocean south of the subcontinent before the directional shift moves north into the Arabian Sea and Bay of Bengal.

7. Phase difference of monsoon onsets over two oceans

If monsoon onsets in the Arabian Sea and the Bay of Bengal are signaled by the change of wind and **Θ** directions, the maps in Fig. 5 show that summer monsoon starts earlier in the Bay of Bengal than in the Arabian Sea, and the phase difference is likely to be the cause of the PMD. We compare 9 years (2007–15) of monsoon onsets relative to rise in SST in the Arabian Sea and the Bay of Bengal. Three years (2007, 2013, and 2015) of the comparisons are shown in Fig. 6 as examples. The zonal component of transport Θ_x, averaged between 10° and 18°N in the Bay of Bengal along 85°E, changes to positive earlier than that in the Arabian Sea along 70°E in all 9 years, resulting in a negative moisture transport into the subcontinent during the time difference. The Θ_x changes to positive (eastward) right after the peak of similarly averaged SST in both the Arabian Sea and the Bay of Bengal. SST also peaks earlier in the Bay of

Bengal than the Arabian Sea. The time lags of change between the two oceans were less for the years 2009 and 2010 (not shown), but there were still deficits of moisture transport into the subcontinent. In 2011 and 2012 (not shown), there were broad periods of warming in the Bay of Bengal, without a sharp peak. In 2015, SST had a broad peak in the Arabian Sea, but a narrow peak in the Bay of Bengal. In all 9 years, SST reached around 30°C, above 27°C, which is the generally recognized threshold to maintain deep convection (e.g., Graham and Barnett 1987) before Θ_x turned positive.

These results are consistent with the analysis of Yu et al. (2012), using in situ measurements in the Bay of Bengal. Although they did not elaborate, the earlier start of SST rise and monsoon wind in the Bay of Bengal than the Arabia Sea could be discerned in the figures presented by Jiang and Li (2011). These two studies are described in section 1. Averages at a single longitude in Fig. 6 may not provide sufficient details. Despite the year-to-year variability, the time difference of monsoon onsets between the two oceans occurs every year as regularly as monsoon onset.

The effects of the PMD may be amplified by the delay of summer monsoon onsets, but 9 years of rainfall and $\boldsymbol{\Theta}$ data show that it occurs whether the onset is early or late. Figure 7 shows the interannual anomalies of monthly data (with the annual cycle compiled from 9 years of data removed) for rainfall integrated over land area and the net $\boldsymbol{\Theta}$ integrated over coastlines. The large positive (2007, 2008, and 2013) and negative (2009, 2012, and 2014) anomalies in June signify early and late monsoon onsets. The PMD occurred in all these years.

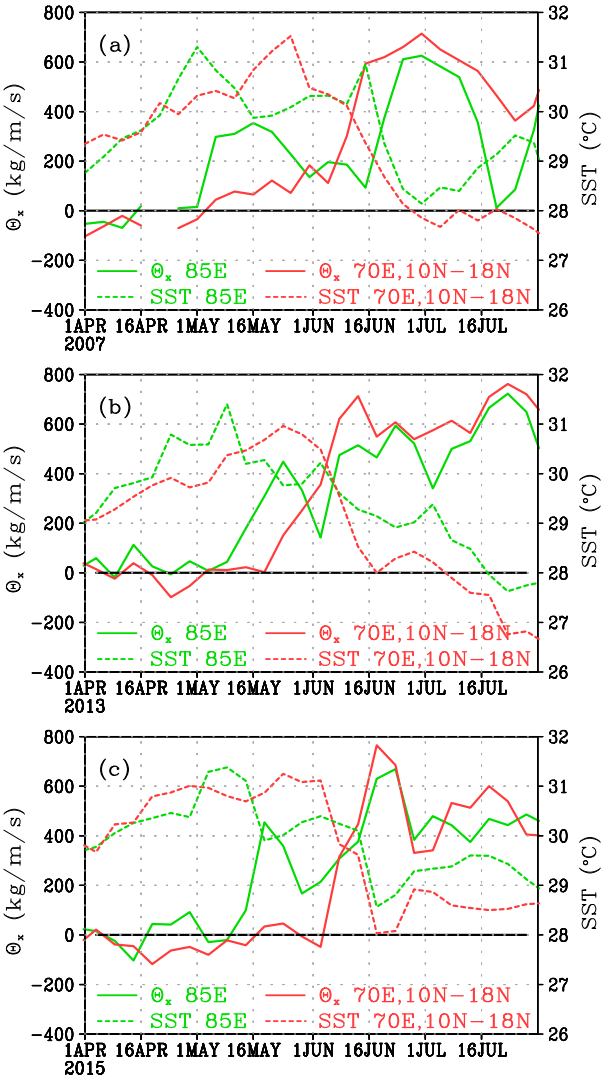

FIG. 6. The zonal component of integrated water transport (solid line) and SST (dashed line) averaged from 10° to 18°N along 85°E in the Bay of Bengal (green), compared with those along 70°E in the Arabian Sea (red), between April and July for (a) 2007, (b) 2013, and (c) 2015.

8. Discussion

New satellite data are exploited to link oceanic and terrestrial water cycles through monsoon. Soil moisture measurement by L-band radiometers identifies the time and location of PMD, in agreement with the reports by news media on fatality, amid the dry season with little persistent rainfall. For all the four monsoon seasons we observed, the PMD includes the hottest and driest week of the year before summer monsoon onsets. Our analysis was enabled by the opportunity to match the PMD timing with those of moisture deficit revealed by $\boldsymbol{\Theta}$. With our space-based $\boldsymbol{\Theta}$ data, we show that the net deficit of $\boldsymbol{\Theta}$ into India from the ocean is caused by the earlier start of summer monsoon winds in the Bay of Bengal than the Arabian Sea. Monsoon wind changes always follow SST rises, and they happen in the Bay of Bengal earlier than the Arabian Sea. Nine years of $\boldsymbol{\Theta}$ data show that there is a $\boldsymbol{\Theta}$ deficit, and therefore the PMD, regardless of whether the monsoon onset is early or late. The short duration of satellite data, however, hampers studies on long-term variability.

While the interannual and decadal variations of monsoon onsets may depend on global atmospheric circulation, our 9 years of data show SST rise consistently precedes wind changes in both the Arabian Sea and the Bay of Bengal. Whether the SST rise sets up its own convection or draws convection clusters from the equatorial ocean is a question to be answered in future studies by atmospheric scientists. Because the SST rise does not follow monsoon-driven ocean current, the cause of their phase difference between the Arabian Sea and the Bay of Bengal and the ocean heat sources

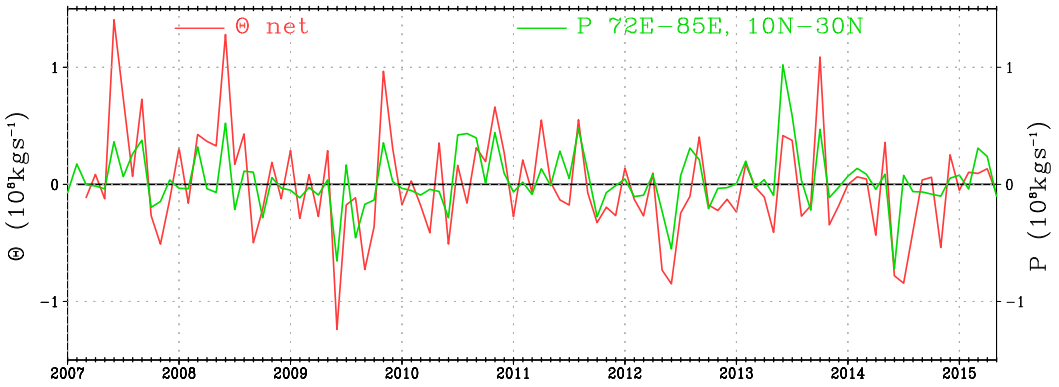

FIG. 7. Time series of net moisture transport from ocean to the Indian subcontinent [**Θ** (red) and precipitation (green)] integrated between 10° and 30°N and 72° and 85°E, with the annual cycle removed.

remain to be addressed by oceanographers. There are several sources of near-real-time SST data products. SST rises precede monsoon onsets in the Bay of Bengal and have the potential to provide advanced warning of the PMD and allow mitigation of its adverse effects. Continuous, consistent, and high quality space-based data are needed to understand longer-period processes.

Acknowledgments. This research was carried out at the Jet Propulsion Laboratory, California Institute of Technology, under a contract with the National Aeronautics and Space Administration (NASA). It was supported by the Precipitation Measuring Mission, Physical Oceanography Program, and Energy and Water Cycle Studies of NASA with contract to both authors. Eni Njoku kindly advised on soil moisture data. We are grateful to Simon Yueh for providing support from the SMAP Project.

REFERENCES

Ananthakrishnan, R., and M. K. Soman, 1988: The onset of the southwest monsoon over Kerala: 1901–1980. *Int. J. Climatol.*, **8**, 283–296, doi:10.1002/joc.3370080305.

Bartalis, Z., W. Wagner, V. Naeimi, S. Hasenauer, K. Scipal, H. Bonekamp, J. Figa, and C. Anderson, 2007: Initial soil moisture retrievals from the *METOP-A* Advanced Scatterometer (ASCAT). *Geophys. Res. Lett.*, **34**, L20401, doi:10.1029/2007GL031088.

Bindlish, R., T. Jackson, M. Cosh, T. Zhao, and P. O'Neill, 2015: Global soil moisture from the *Aquarius/SAC-D* satellite: Description and initial assessment. *IEEE Geosci. Remote Sens. Lett.*, **12**, 923–927, doi:10.1109/LGRS.2014.2364151.

Chahine, M. T., and Coauthors, 2006: AIRS: Improving weather forecasting and providing new data on greenhouse gases. *Bull. Amer. Meteor. Soc.*, **87**, 911–926, doi:10.1175/BAMS-87-7-911.

Chang, C. P., and T. N. Krishnamurti, 1987: *Monsoon Meteorology. Oxford Monogr. on Geology and Geophysics*, No. 7, Oxford University Press, 344 pp.

Dai, A., K. E. Trenberth, and T. Qian, 2004: A global dataset of Palmer drought severity index for 1870–2002: Relationship with soil moisture and effect of surface warming. *J. Hydrometeor.*, **5**, 1117–1130, doi:10.1175/JHM-386.1.

Dawadi, B., E. Liang, L. Tian, L. P. Devkota, and T. Yao, 2013: Pre-monsoon precipitation signal in tree rings of timberline *Betula utilis* in the central Himalayas. *Quat. Int.*, **283**, 72–77, doi:10.1016/j.quaint.2012.05.039.

Entekhabi, D., and Coauthors, 2010: The Soil Moisture Active Passive (SMAP) mission. *Proc. IEEE*, **98**, 704–716, doi:10.1109/JPROC.2010.2043918.

——, N. Das, E. Njoku, S. Yueh, J. Johnson, and J. Shi, 2014: L2 & L3 radar/radiometer soil moisture (active/passive) data products. Algorithm Theoretical Basis Doc., Jet Propulsion Laboratory, 89 pp.

Fasullo, J., and P. J. Webster, 2003: A hydrological definition of Indian monsoon onset and withdrawal. *J. Climate*, **16**, 3200–3211, doi:10.1175/1520-0442(2003)016<3200a:AHDOIM>2.0.CO;2.

Gadgil, S., 2003: The Indian monsoon and its variability. *Ann. Rev. Earth Planet. Sci.*, **31**, 429–467, doi:10.1146/annurev.earth.31.100901.141251.

——, M. Rajeevan, and P. A. Francis, 2007: Monsoon variability: Links to major oscillations over the equatorial Pacific and Indian Oceans. *Curr. Sci.*, **93**, 182–194.

Graham, N. E., and T. P. Barnett, 1987: Sea surface temperature, surface wind divergence, and convection over tropical oceans. *Science*, **238**, 657–659, doi:10.1126/science.238.4827.657.

Guttman, N. B., 1999: Accepting the standardized precipitation index: A calculation algorithm. *J. Amer. Water Resour. Assoc.*, **35**, 311–322, doi:10.1111/j.1752-1688.1999.tb03592.x.

Hilburn, K. A., 2010: Intercomparison of water vapor transport datasets. *17th Conf. on Satellite Meteorology and Oceanography/17th Conf. on Air–Sea Interaction*, Annapolis, MD, Amer. Meteor. Soc., JP1.4. [Available online at https://ams.confex.com/ams/17Air17Sat9Coas/techprogram/paper_175150.htm.]

Huffman, G. J., and Coauthors, 2007: The TRMM Multisatellite Precipitation Analysis (TMPA): Quasi-global, multiyear, combined-sensor precipitation estimates at fine scales. *J. Hydrometeor.*, **8**, 38–55, doi:10.1175/JHM560.1.

——, D. T. Bolvin, D. Braithwaite, K. Hsu, R. Joyce, and P. Xie, 2014: NASA Global Precipitation Measurement Integrated Multi-satellitE Retrievals for GPM (IMERG). Algorithm Theoretical Basis Doc., version 4.4, 30 pp. [Available online at https://pps.gsfc.nasa.gov/Documents/IMERG_ATBD_V4.pdf.]

Jackson, T. J., and Coauthors, 2010: Validation of Advanced Microwave Scanning Radiometer soil moisture products. *IEEE Trans. Geosci. Remote Sens.*, **48**, 4256–4272, doi:10.1109/TGRS.2010.2051035.

——, and Coauthors, 2012: Validation of Soil Moisture and Ocean Salinity (SMOS) soil moisture over watershed networks in the U.S. *IEEE Trans. Geosci. Remote Sens.*, **50**, 1530–1543, doi:10.1109/TGRS.2011.2168533.

Jiang, X., and J. Li, 2011: Influence of annual cycle of sea surface temperature on the monsoon onset. *J. Geophys. Res.*, **116**, D10105, doi:10.1029/2010JD015236.

Lau, K. M., and S. Yang, 1997: Climatology and interannual variability of the Southeast Asian summer monsoon. *Adv. Atmos. Sci.*, **14**, 141–162, doi:10.1007/s00376-997-0016-y.

Li, K., and Coauthors, 2012: Structure and mechanisms of the first-branch northward-propagating intraseasonal oscillation over the tropical Indian Ocean. *Climate Dyn.*, **40**, 1707–1720, doi:10.1007/s00382-012-1492-z.

Li, L., and Coauthors, 2010: WindSat global soil moisture retrieval and validation. *IEEE Trans. Geosci. Remote Sens.*, **48**, 2224–2241, doi:10.1109/TGRS.2009.2037749.

Liu, W. T., and W. Tang, 2005: Estimating moisture transport over ocean using space-based observations from space. *J. Geophys. Res.*, **110**, D10101, doi:10.1029/2004JD005300.

——, and X. Xie, 2014: Ocean–atmosphere water flux and evaporation. *Encyclopedia of Remote Sensing*, E. G. Njoku, Ed., Springer, 480–489, doi:10.1007/978-0-387-36699-9_122.

——, ——, and W. Tang, 2005: Monsoon, orography, and human influence on Asian rainfall. *Proc. First Int. Symp. on Cloud-Prone and Rainy Areas Remote Sensing*, Hong Kong, China, Chinese University of Hong Kong, 7 pp. [Available online at http://airsea.jpl.nasa.gov/publication/paper/CARRS-ms5.pdf.]

——, ——, ——, and V. Zlotnicki, 2006: Spacebased observations of oceanic influence on the annual variation of South American water balance. *Geophys. Res. Lett.*, **33**, L08710, doi:10.1029/2006GL025683.

——, ——, and K. B. Katsaros, 2012: Observation of oceanic origin of Sahel precipitation from space. *Remote Sens. Environ.*, **123**, 593–599, doi:10.1016/j.rse.2012.04.007.

Naeimi, V., Z. Bartalis, and W. Wagner, 2009: ASCAT soil moisture: An assessment of the data quality and consistency with the ERS scatterometer heritage. *J. Hydrometeor.*, **10**, 555–563, doi:10.1175/2008JHM1051.1.

Pal, I., and A. Al-Tabbaa, 2009: Trends in seasonal precipitation extremes—An indicator of 'climate change' in Kerala, India. *J. Hydrol.*, **367**, 62–69, doi:10.1016/j.jhydrol.2008.12.025.

Ramage, C. S., 1971: *Monsoon Meteorology*. Academic Press, 296 pp.

Thomas, J., and V. Prasannakumar, 2016: Temporal analysis of rainfall (1871–2012) and drought characteristics over a tropical monsoon–dominated state (Kerala) of India. *J. Hydrol.*, **534**, 266–280, doi:10.1016/j.jhydrol.2016.01.013.

Wang, B., H. Lin, Y. Zhang, and M. M. Lu, 2004: Definition of South China Sea monsoon onset and commencement of the East Asia summer monsoon. *J. Climate*, **17**, 699–710, doi:10.1175/2932.1.

Webster, P. J., Y. O. Magana, T. N. Palmer, J. Shukla, R. A. Tomas, M. Yanai, and T. Yasuari, 1998: Monsoons: Processes, predictability, and the prospects for prediction. *J. Geophys. Res.*, **103**, 14 451–14 510, doi:10.1029/97JC02719.

Wentz, F. J., P. D. Ashcroft, and C. L. Gentemann, 2001: Post-launch calibration of the TRMM Microwave Imager. *IEEE Trans. Geosci. Remote Sens.*, **39**, 415–422, doi:10.1109/36.905249.

Xie, X., W. T. Liu, and B. Tang, 2008: Spacebased estimation of moisture transport in marine atmosphere using support vector machine. *Remote Sens. Environ.*, **112**, 1846–1855, doi:10.1016/j.rse.2007.09.003.

Yu, W.-D., J.-W. Shi, L. Liu, K.-P. Li, Y.-L. Liu, and H.-W. Wang, 2012: The onset of the monsoon over the Bay of Bengal: The observed common features for 2008–2011. *Atmos. Ocean. Sci. Lett.*, **5**, 314–318, doi:10.1080/16742834.2012.11447009.